Journal of Information System and Technology Management
JISTM
EISSN: 0128-1666
Volume 7 Issue 29 (December 2022) PP. 10-23
DOI: 10.35631/JISTM.729002

JOURNAL OF INFORMATION SYSTEM AND TECHNOLOGY MANAGEMENT
(JISTM)
www.jistm.com

ANALYSIS OF PERMANENT MAGNETIC-BASED CLIMBING ROBOT DESIGN FOR SHIP HULL AND OIL TANK SERVICES

Muhammad Ammar Nor Azman[1], Muhammad Zulkarnain Zakaria[1], Zulkifli Zainal Abidin[1], Ahmad Imran Ibrahim[1], Mohd Nazli Mohd Salim[2], Muttaqqin Abu Yamin[2], Marmeezee Mohd Yusoff[1]

[1] Centre for Unmanned Technologies (CUTe), Kulliyyah of Engineering, International Islamic University Malaysia, Gombak, 53100 Kuala Lumpur, Malaysia
[2] Marine Solution, Altus Oil & Gas Malaysia Sdn Bhd, Wilayah Persekutuan, 60000 Kuala Lumpur, Malaysia
* Corresponding Author (marmeezee@iium.edu.my)

Article Info:

Article history:
Received date: 15.09.2022
Revised date: 24.10.2022
Accepted date: 17.11.2022
Published date: 01.12.2022

To cite this document:

Azman, M. A. N., Zakaria, M. Z., Abidin, Z. Z., Ibrahim, A. I., Salim, M. N. M., Yamin, M. A., & Yusoff, M. M. (2022). Analysis Of Permanent Magnetic-Based Climbing Robot Design For Ship Hull And Oil Tank Services. *Journal of Information System and Technology Management, 7* (29), 10-23.

DOI: 10.35631/JISTM.729002

Abstract:

Servicing operations in the marine and oilfield industries cover a wide range of tasks, including the removal of biofoulings from ship surfaces, re-painting, and inspection of ship and oil tank surfaces, as both are exposed to the environment. With the rate at which technology has advanced, a modern solution to this challenge may be attainable in assisting manual labour. This paper outlines the development of a robot that climbs a wall at an angle adopting a permanent magnet as the primary adhesion mechanism. Attachable and detachable permanent magnets are used in the robot design to demonstrate how the increments of magnet number affect the climbing of the robot at an angle. The analysis of this experiment includes static and dynamic movement of the robot and a discussion related to the experiment is included in the paper.

Keywords:

Wall Climbing Robot, Permanent Magnet, Adhesion Mechanism, Climbing Angle

Introduction

The demands of engaging people as a key source in cleaning and inspecting a ship's hull and oil tanks were a frequent practice in the early days of service operation in the Marine and Oilfield industries. Implementing cleaning and inspection services in the industries demands

Journal of Information System and Technology Management
EISSN: 0128-1666
Volume 7 Issue 29 (December 2022) PP. 10-23
DOI: 10.35631/JISTM.729002

working at heights or underwater. Scaffoldings, for example, were to be installed a few days before the operations began so that employees could clean and inspect the surface of a ship and oil tanks thoroughly (M. Eich, 2011). In addition to the cleaning and inspection challenges, servicing a ship's hull demands the use of trained divers and the use of a brush cart to remove biofoulings from the hull surface (Han, 2021). This so-called manual operation can have a considerable impact on servicing operations, since the process might cause delays in the project due to human limitations, reducing the overall efficiency of the operation. In terms of costs, docking and anchoring a ship in a port come with their own set of fees, which may include additional charges if the ship is docked for an extended period. In light of this, a collaboration between International Islamic University Malaysia (IIUM) and Altus Oil and Gas Malaysia (AOGM) Sdn. Bhd. has agreed to attempt to develop a concept design to solve these obstacles.

In required to address the challenge, many climbing robots have been widely used in the industry, with adhesion technologies such as magnets, suction pads, and propellers being used to adhere to a vertical surface. One of the most important aspects of operating a wall-climbing robot is ensuring the robot's adhesion efficiency so that the service operations are not disrupted. Factors such as wet surface, curvy surface, and surface obstacles (barnacles, pipes, cracks, etc.) will obstruct the adhesion of a wall-climbing robot (Albitar, 2016).

According to V. Prabakaran (2020), D. Souto (2013) and F. Ortiz (2007), a fixed adhesion system with a specific function, such as water blasting, is common in commercialized cleaning and inspection robots. This leads to an additional cost to purchase a different type of robot to execute a different type of task. The proposed robot design that we develop uses permanent magnets as the main adhesion mechanism. The goal of this research is to investigate the concepts of locomotion, robot mechanism, and permanent magnetic approach for robot adhesion system while keeping the changeable attachments in consideration.

Related Research

The permanent magnet detailed by Xu (2015) demonstrates that permanent magnets come in a variety of types and sizes. Ceramic, Alnico, Neodymium Iron Boron (NdFeB), Samarium Cobalt (SmCo), and Neodymium Iron Boron (NdFeB) are some of the materials used. Each permanent magnet material has its own unique set of properties. According to the discussion, Neodymium Iron Boron (NdFeB) is the permanent magnet with the highest adhesion force and the most suited features for the robot. NdFeB has its own grade scale, ranging from N35 to N54. The permanent magnetic adhesion mechanisms have issues with cancelling the attraction force in order to release the robot from ferrous surfaces. This is due to the adhesion force of the permanent magnet being fixed and cannot be adjusted. There have been few related discussions and designs to counter this problem.

In order to find a solution, it was suggested that an adsorption-force-changeable permanent magnetic unit be used (Lee, 2013). With a six-degree-of-freedom locomotive concept, the mechanism is made up of a permanent magnet unit, a magnet lifting mechanism, and a force sensor. The design was effectively built for three separate states. First, there's the full adhesion state, which maintains the maximal magnetic force. Second, is the moving state in which the magnet is partially lifted but still maintains a sufficient adsorption force to allow a robot to attach to a surface. The third stage is a free state, in which no magnetic force is needed, and the magnet is lifted away from the surface.

Journal of Information System and Technology Management
JISTM
EISSN: 0128-1666
Volume 7 Issue 29 (December 2022) PP. 10-23
DOI: 10.35631/JISTM.729002

Another technique to use a permanent magnet for an adhesion mechanism is to make a magnetic wheel. This is a popular way to adapt a permanent magnet onto a wall-climbing robot. This approach uses a container-like concept, in which a permanent magnet is positioned inside a custom-made housing in such a way that it maintains constant contact with a ferrous surface (Ishihara, 2017) and (Cai, 2017). A few factors will need to be considered in the design, such as the rim design, tyre pattern design, and the distance between the magnet and the surface.

Some other method is to alter the permanent magnets' polarities, by using 2 magnets (K. Yoon, 2012) and (M. Tavakoli, 2015). One magnet is fixedly attached to a robot surface while the second magnet is attached on top of the fixed magnet. The second magnet is able to rotate at horizontal axis. When no adhesion force is required, the poles are positioned antiparallel, which implies that the magnetic flux is directed toward the fixed permanent magnets. The magnets will be arranged parallel in an adhesive state, causing the magnetic flux to point out to the surface.

The magnetic flux itself may be influenced by the arrangement of magnets. If two magnets are placed together at a close distance, the magnetic field may be disturbed, reducing the total adhesion force of the magnets. According to Faruq Howlader (2015), the total adhesion force increases as the distance between magnets increases until it reaches a peak before the adhesion force started to gradually decrease again. As a result, the positioning of the magnets must be considered in order to get the optimum adhesion force for the magnets.

The robot design in this paper uses attachable permanent magnets, with the number of permanent magnets used increasing as the inclination of the plate rises. This is to demonstrate an experimental setup in which the robot adhesion force can be studied using a permanent magnet. The next section will go into the details of the robot's design.

Modelling, Robot Design and System Architecture

Force Analysis

To ensure that the robot can compromise vertical climbing while preventing slippage, the modelling for the robot force analysis must be studied. Since the robot relies exclusively on adhesion force to prevent slippage, it is necessary to guarantee that the adhesion force is strong enough to prevent slipping. This modelling will incorporate a few parameters that are thought to influence the robot adhesion force. The gravity will be represented by $\boldsymbol{g}$, and the robot mass will be represented by $\boldsymbol{m}$. The friction force will be represented by $\boldsymbol{F_f}$, while the adhesive force will be represented by $\boldsymbol{F_A}$. Last is the coefficient friction which will be represented as $\boldsymbol{\mu}$. Figure 1(a) shows the free body diagram of the robot with all the related force at rest on a level surface.

Journal of Information System and Technology Management
JISTM
EISSN: 0128-1666
Volume 7 Issue 29 (December 2022) PP. 10-23
DOI: 10.35631/JISTM.729002

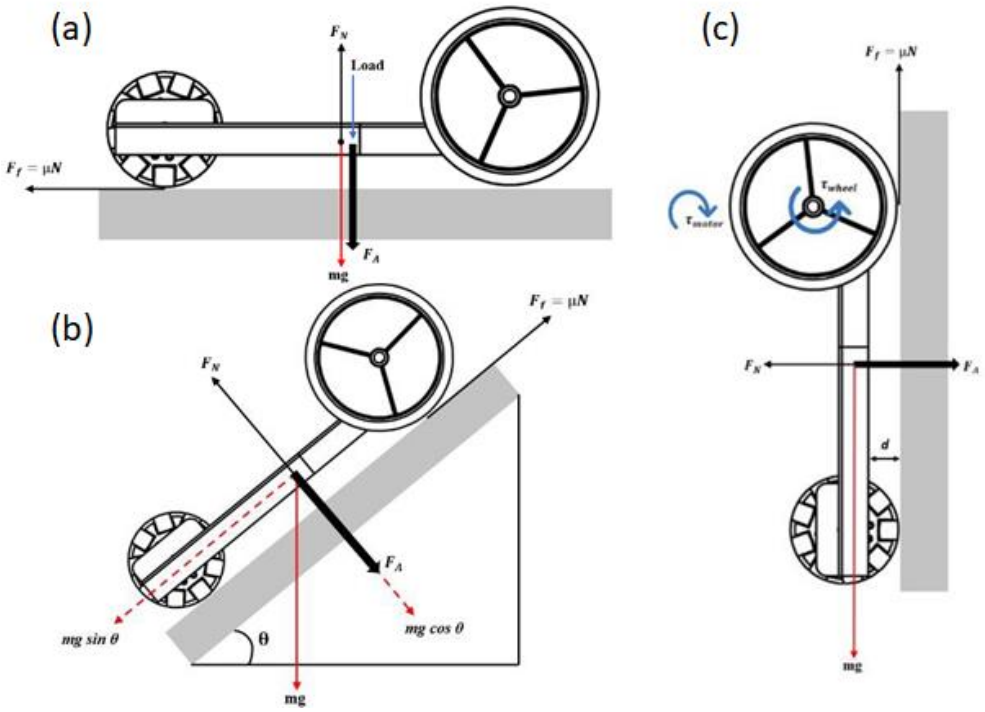

Figure 1: Free Body Diagram of the Robot (a) at Rest on Level Surface, (b) on Inclination Surface and (c) on Vertical Plane with Labelled Torque and Force.

To further analyse the relationship between the angle plane and the adhesion force, it is represented as following free body diagram in Figure 1 (b). Equation (1) depict the force on x-axis and Equation (2) depict the force on y-axis. The equation (1) and (2) is related to by the normal force, $\boldsymbol{F_N}$ represented in equation (3).

Force on x-axis:

$$\sum F_{x-axis} = \frac{mg \sin\theta}{\mu} \tag{0}$$

$$F_N = \frac{mg \sin\theta}{\mu} \tag{1}$$

Force on y-axis:

$$\sum F_{y-axis} = mg \cos\theta + F_A \tag{2}$$

Thus, the relation between the two equations:

$$\frac{mg \sin\theta}{\mu} = mg \cos\theta + F_A \tag{3}$$

Journal of Information System and Technology Management
EISSN: 0128-1666
Volume 7 Issue 29 (December 2022) PP. 10-23
DOI: 10.35631/JISTM.729002

Condition (4) must be fulfilled to avoid robot slippage:

$$F_A > \left[\left(\frac{mg \sin\theta}{\mu}\right)\right] - mg\cos\theta \quad (4)$$

At θ = 90°, use (5) as the condition and at θ = 180° use (6). If the robot is not at rest or in moving condition, the equation need to be added with another force as in (7). $\boldsymbol{a}$ represents the acceleration of the robot.

$$F_A > \frac{mg}{\mu} \quad (5)$$

$$F_A > mg \quad (6)$$

$$F_A > \frac{(mg + ma)}{\mu} \quad (7)$$

Wheel roll-over can happen as a result of the wheel and gravity. Figure 1 (c) shows how the torque from the wheel causes the robot to travel backwards. As a result, the torque of the motor should be greater than the torque of the wheel to avoid slipping. The torque of the wheel is calculated by using (8). The required torque for the motor may then be calculated using (9).

$$\tau_{wheel} = F_f * r = \mu F_N * r \quad (8)$$

$$\tau_{motor} = (mg * d) + (\mu F_N * r) \quad (9)$$

Robot Design

As illustrated in Figure 2, the robot is designed with a differential drive system, in which two front wheels are operated independently by a 18V DC motor connected to a motor driver. The driving systems assist the robot in changing directions by individually controlling the speed of each wheel. For example, in order to drive forward, both wheels must rotate in the same direction at the same speed. The weight of the experiment robot is 7.38kg.

Journal of Information System and Technology Management
JISTM
EISSN: 0128-1666
Volume 7 Issue 29 (December 2022) PP. 10-23
DOI: 10.35631/JISTM.729002

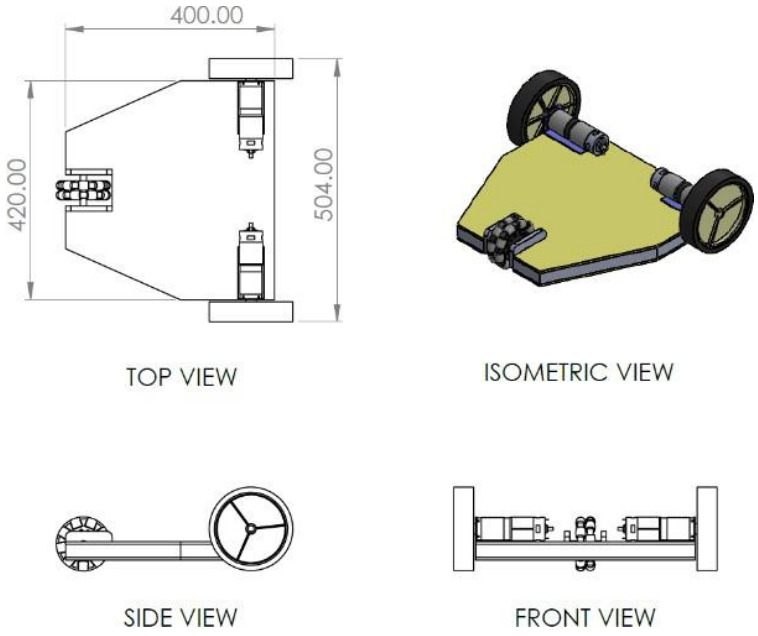

Figure 2: Robot Design Drawing with Top View, Isometric View, Side View and Front View.

The material used to build the main body frame of the robot is made out of mild steel where we fabricated it at the size of 400mm x 420mm x 25.40mm. To reinforce the main body frame, the mild steel has been welded to each other. A pair of acrylic sheets is mounted on the top and the bottom side of the robot body frame.

The wheel must also go through the selecting procedure. When choosing the radius of the wheel, the minimum distance between the magnet at the bottom of the robot body and the wall surface must be considered. Since the motor will be at the top of the body, the wheel's radius should be calculated from the motor to the bottom section of the body. The radius of the wheel is expected to be 75mm. The wheel should be made of rubber because it requires more grip, particularly while climbing an inclination plane or vertical wall. The diameter of the driven wheel must conform to the first criteria. Its radius can be varied or different from the drive wheels, but it must not interfere with the 10 mm space between the lower body and the wall surface. The Omni wheel was chosen as the driving wheel because it can move in multiple directions, which aids in robot steering.

Magnet Types and Distribution

There are two types of magnets used in this robot: ferrite and neodymium magnets. The characteristics of these two magnets are shown in Table I. Neodymium is the most powerful magnet material available, based on both characteristics. It can be used in applications that require a high of flux density. Because the shapes of these two magnets differ, it is expected that their magnetic fields will differ. Neodymium magnet act as the main adhesion force of the robot meanwhile ferrite magnet will act as supporting adhesion force that can be added when needed. Table II listed down all the specification of these two magnets that will be used for the robot.

Journal of Information System and Technology Management
JISTM
EISSN: 0128-1666
Volume 7 Issue 29 (December 2022) PP. 10-23
DOI: 10.35631/JISTM.729002

Table I. Characteristics of Neodymium and Ferrite Magnets

Characteristics	Ferrite	Neodymium
Flux Density (Gauss)	1000	4500
Max Energy Product: SI, Kj/ m^3	26	279
Maximum Working Temperature, ˚C	250	80
Resistance to Demagnetization	High	Very High
Corrosion Resistance Uncoated	Excellent	Poor

Table II. Magnet Specifications

Magnet Specifications	Ferrite	Neodymium
Diameter, mm	50	-
Thread	M8	2 x M3
Thickness, mm	10	5
Weight, g	160	28
Pull Force, kg	15	30
Length, mm	-	60
Width, mm	-	13.5

The magnetic field between the magnets may be disrupted by the positioning of the magnets. There is a possibility that the magnetic fields will cancel each other out. Although the magnet's pulling force is sufficient, it can be weakened if the magnet's position is not carefully considered. Using Finite Element Method Magnetics (FEMM) software, simulations were run to determine the magnetic field of the magnets. Figure 3 (left) depicts a simulation of the neodymium magnet bar's magnetic field and flux density. The flux density is much higher in the magnet's centre or body, and the magnetic field in and out from the magnet bar's tips.

Figure 3 (right) illustrates the magnetic field produced by a circular ferrite magnet. According to the diagram, the magnetic field of the neodymium magnet bar is not significantly different. The flux density is substantially higher in the magnet's core or body. As a result, it is inferred that magnets require a space between them in order to exert their full pulling force.

Journal of Information System and Technology Management
JISTM
EISSN: 0128-1666
Volume 7 Issue 29 (December 2022) PP. 10-23
DOI: 10.35631/JISTM.729002

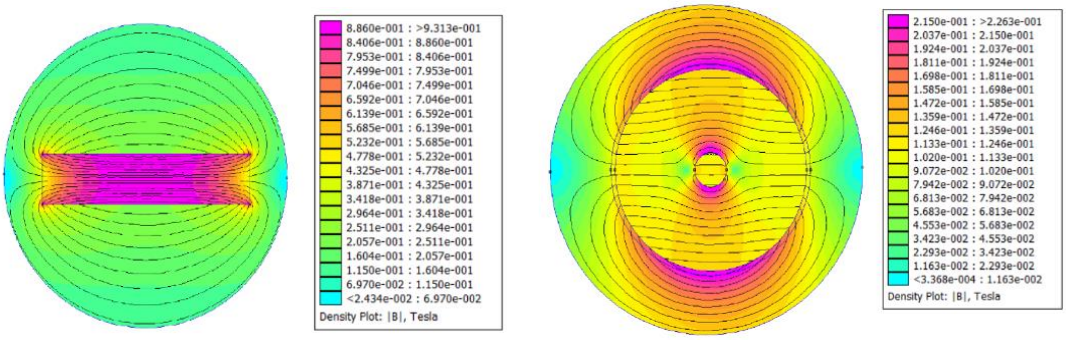

Figure 3: (left) Neodymium Bar Magnet Magnetic Field and Flux Density, and Figure 3: (right) Ferrite Magnet Magnetic Field and Flux Density.

The adhesion force must be distributed according to the robot's required force to fully adhere the robot to a surface. In this situation, adhesion force is critical near the motor and driving wheels, which are located towards the robot's front end. To counteract the roll-over effect, more magnets will be positioned towards the bottom of the motor position. Several magnets were placed on the robot's back to help it become more stable and prevent the omni-wheel from flipping over. Figure 4 displays the positions of the magnets and FEMM stimulation to show the flux density of the magnetic field.

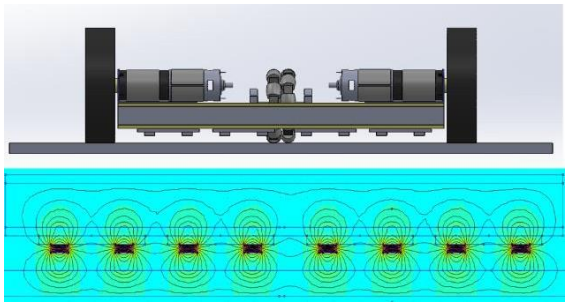

Figure 4: Magnet Position and Distribution on Wall Climbing Robot.

System Architecture

The electronics are made up of two sections. The first set of parts is placed on the control block, followed by the second set of parts on top of the robot. Power supply, selector switch, panel LED lamp, Raspberry Pi 4, controller, keyboard, and desktop are all parts that go on the control block. The Raspberry Pi 4 and power supply will be powered by the socket's AC voltage. The Raspberry Pi 4 will serve as the system's microprocessor. The application will run on a Raspberry Pi 4 with an Arduino Mega linked to it. The robot's motor drivers, motors, and Arduino were all mounted on top of the robot. The Arduino will be powered on by connecting it to the Raspberry Pi 4 through a five-meter wired USB cable. The power supply will provide power to the motor drivers and motors. The user can use the selector switch to turn on the motors and motor drivers. Robot are controlled manually thus no sensors are included in the system. Figure 5 illustrates the system architecture of the robot control system.

Journal of Information System and Technology Management
JISTM
EISSN: 0128-1666
Volume 7 Issue 29 (December 2022) PP. 10-23
DOI: 10.35631/JISTM.729002

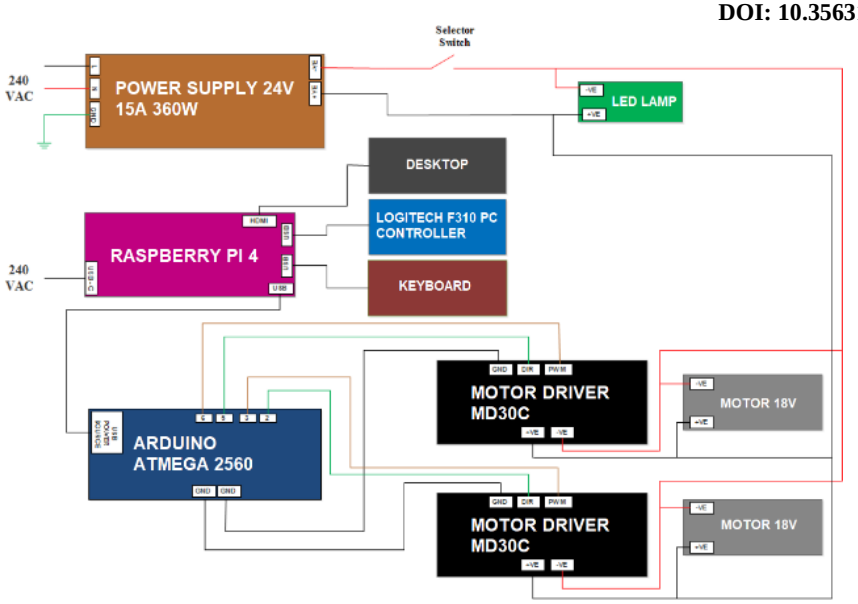

Figure 5: Full Drive System Connection Circuits for The Robot.

Experiment Analysis and Results

Experimental Setup and Procedure

The proposed method was applied using a custom adjustable angular mild steel plate for the experiment environment. This plate is use to imitate the surface of a ship hull with 15mm thickness. With the size of 1000mm x 1200mm, the plate gives a sufficient room to manoeuvre the robot. The plate is place onto a mounting frame with a pulley system that is attached to the side of frame. The pulley line is anchored to the mild steel plate using winch rope at top side of the plate to adjust the angle.

The plate will then be adjusted to increase the inclination of the plate until the robot detach from the mild steel plate. The drawbacks of this setup are that the maximum vertical plane angle can only reach up to 73.75˚ due to the fixed hook attached on the mild steel plate. Table III displays a few parameters that are employed in the equation (4) to compute the Adhesion Force, *FA*. It should be noted that MATLAB was used to generate all of the graphs.

Table III. Parameters of Robot

Parameters	Value
m	7.38kg
g	9.81
r	75mm
μ	0.8
θ	0 -180˚
d	10mm
a	0.5m/**s**^{2}

Journal of Information System and Technology Management
EISSN: 0128-1666
Volume 7 Issue 29 (December 2022) PP. 10-23
DOI: 10.35631/JISTM.729002

Maximum Angle against Number of Magnets

The measurement of the maximum angle is recorded using digital angle gauge for every additional number of magnets attached to the robot base. Once the number of neodymium magnets reaches 9, ferrite magnets will be used as an additional support adhesion. Maximum angle measurements are conducted in two conditions: static state and dynamic state. Noted that the data for the dynamic state will only be recorded when the robot has successfully moved on the plate steadily.

Table IV. Recorded Data for Maximum Angle (˚) Climbing

Number of Magnet	Maximum Angle (˚) Climbing	
	Static	***Dynamic***
2	26.80	24.50
3	26.80	33.85
4	34.00	36.50
5	54.50	37.40
6	58.10	45.20
7	64.05	53.90
8	73.75	63.50
9	128.00	73.75
73.75° is the maximum angle for inclined plane. 106.25° is the starting angle for upside down plane. Beyond this point, magnets that will be added is ferrite magnet.		
10	140.00	73.75
11	180.00	73.75
12	180.00	73.75
13	-	73.75
14	-	106.25
15	-	180.00
16	-	180.00

As shown in Figure 6, increasing the number of magnets is extremely beneficial in improving the adhesion force and maximum climbing angle. It has been shown that the maximum angle increases linearly as the number of magnets increases. In comparison to angles at the horizontal point, angles near the vertical point demand more adhesive force.

Table IV demonstrates that in the static state, the robot only requires 12 magnets to ensure that it can attach to a surface at an angle of 180° without slipping. In contrast to the static state, the dynamic state requires an additional 3 magnets to firmly adhere to 180°. As a result, greater adhesive force is required to ensure that the robot can travel steadily on an inclined plane in a dynamic state.

Journal of Information System and Technology Management
JISTM
EISSN: 0128-1666
Volume 7 Issue 29 (December 2022) PP. 10-23
DOI: 10.35631/JISTM.729002

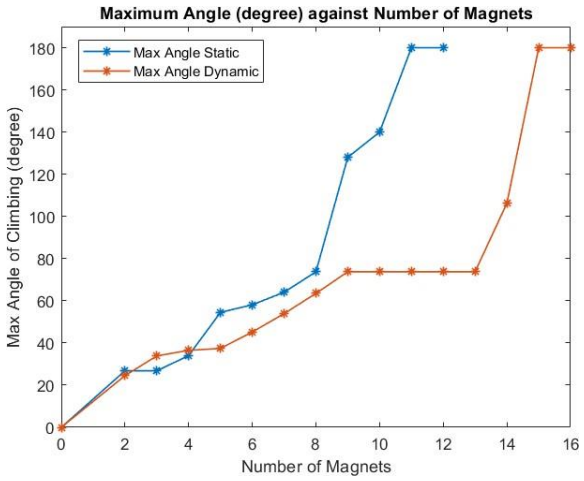

Figure 6: Maximum Angle with Respect to Number Of Magnets.

In the first test, the robot was mounted at a 45° angle, as shown in Figure 7 (a). Figure 7 (b) shows how the robot succeeded to adhere at the plate's maximum vertical angle, which is 73.75°. Further discussion is made at starting of upside-down angle which is 106.25˚. The robot is mounted to the plate surface at an upside-down angle shown Figure 8 (a). The robot was then put through its tests with increasing numbers of magnets until it reached its maximum angle of 180° as shown in Figure 8 (b). The robot was able to attach to the surface plate at varied angles without difficulty.

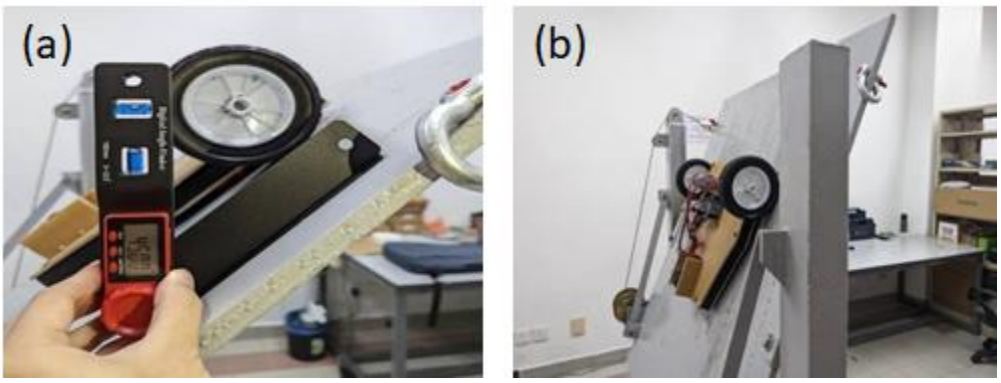

Figure 7: (a) The Robot Attached on Inclined Surface at Angle 45°. (b) The Robot Attached on Maximum Vertical Angle of the Plane.

Journal of Information System and Technology Management
JISTM
EISSN: 0128-1666
Volume 7 Issue 29 (December 2022) PP. 10-23
DOI: 10.35631/JISTM.729002

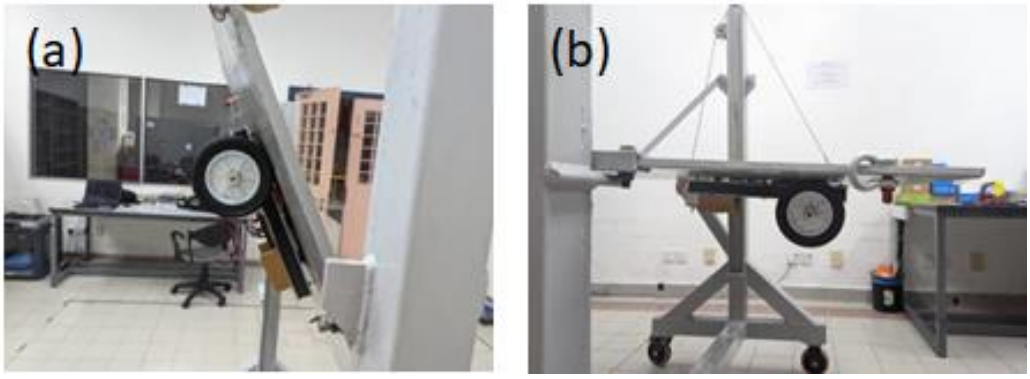

Figure 8: (a) The Robot Attached onto the Plane at Upside Down Angle. (b) The Robot Attached onto the Plane at 180° Upside Down.

Comparison between Experiment and Stimulated Adhesion Force

The adhesion force for the robot will be calculated using the data from the recorded maximum angle. The adhesion force data will comprise both static and dynamic states, as in the previous section. The adhesive force for the dynamic state was determined by multiplying the robot's mass by its acceleration which is added to equation (4). The result is then represented in table 5 and graphed.

Table V. Recorded Data for Adhesion Force

Number of Magnet	Maximum Angle (˚) Climbing		
	Static	***Dynamic***	***Calculated***
2	0.66	125.92	2.71
3	0.66	140.78	22.79
4	20.94	144.33	42.17
5	75.83	145.46	60.28
6	84.66	153.76	76.55
7	98.51	159.65	90.49
8	118.70	161.89	101.69
9	158.60	159.27	109.80
73.75° is the maximum angle for inclined plane. 106.25° is the starting angle for upside down plane. Beyond this point, magnets that will be added is ferrite magnet.			
10	148.50	159.27	114.57
11	72.39	159.27	115.86
12	72.39	159.27	113.63
13	-	159.27	107.95
14	-	118.75	98.98
15	-	72.40	87.01
16	-	72.40	72.39

Journal of Information System and Technology Management
EISSN: 0128-1666
JISTM
Volume 7 Issue 29 (December 2022) PP. 10-23
DOI: 10.35631/JISTM.729002

Figure 9 represents the relationship between minimum adhesive force and the maximum angle of climbing. MATLAB was used to calculate a stimulated adhesion force using an identical dynamic state equation and the same parameters. The maximum adhesion force for all graphs follows a similar pattern. The adhesion force started at above 120N and reaches the highest value of adhesion force required is 161.89N at 63.5˚ before decreasing to the most maximum angle which at 180°. As there are so many external influences that might affect the robot, making it move steadily on an inclined plane is considerably more difficult. Tire grip, acceleration, change in distance between magnets and surface, and wheel alignment are all factors that can affect the robot's stability. As a result, our results differ from those of the previous study.

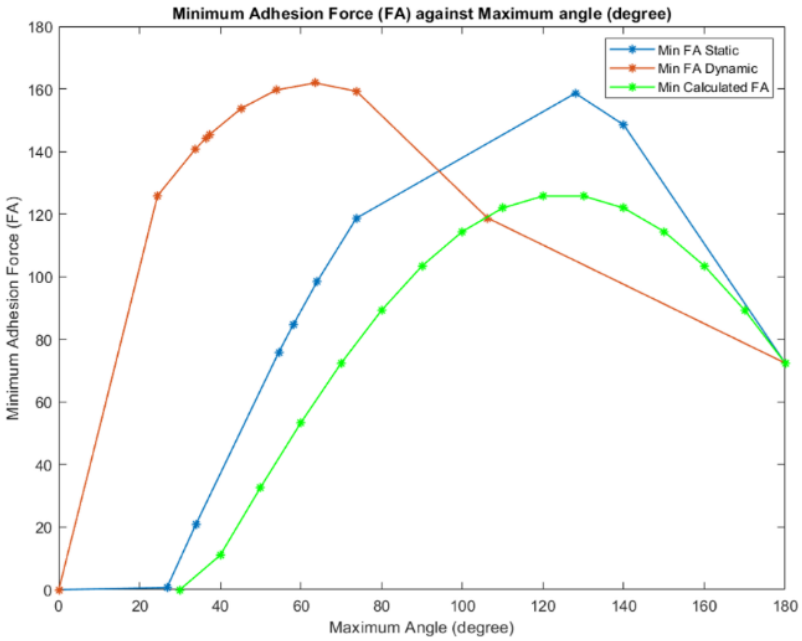

Figure 9: Minimum Adhesion Force Against Maximum Angle

Conclusion

This paper proposes a permanent magnet approach for wall climbing robots, which involves increasing the number of magnets and analysing the adhesion force and maximum climbing angle. By increasing the number of magnets, this type of adhesion technology is able to provide a high adhesion force. Several modifications could be made to improve the robot's overall performance and prepared it to confront new challenges in the near future.

Acknowledgement

The author wishes to express his gratitude to all parties who were directly or indirectly involved in this effort, particularly the IIUM Centre for Unmanned Technologies (CUTe) lab for providing equipment. This initiative was also made possible by the community of IIUM and AOGM's unwavering support.

References

Albitar, H., Dandan, K., Ananiev, A., & Kalaykov, I. (1 January, 2016). Underwater Robotics: Surface Cleaning Technics, Adhesion and Locomotion Systems. International Journal of Advance Robotic Systems. doi:https://doi.org/10.5772/62060

Journal of Information System and Technology Management
EISSN: 0128-1666
JISTM
Volume 7 Issue 29 (December 2022) PP. 10-23
DOI: 10.35631/JISTM.729002
Cai, J., He, K., Fang, H., & Maxwell, A. (2017). The Design of Permanent-Magnetic Wheeled Wall- Climbing Robot. July, 604–608.

D. Souto, A. Faiña, F. López-Peña and R. J. Duro, "Lappa: A new type of robot for underwater non-magnetic and complex hull cleaning," 2013 IEEE International Conference on Robotics and Automation, 2013, pp. 3409-3414, doi: 10.1109/ICRA.2013.6631053.

F. Ortiz et al., "Robots for hull ship cleaning," 2007 IEEE International Symposium on Industrial Electronics, 2007, pp. 2077-2082, doi: 10.1109/ISIE.2007.4374928.

Faruq Howlader, M. O., & Sattar, T. P. (2015). Development of magnetic adhesion based climbing robot for non-destructive testing. 2015 7th Computer Science and Electronic Engineering Conference, CEEC 2015 - Conference Proceedings, 105–110. https://doi.org/10.1109/CEEC.2015.7332708

Han, Cong & Qu, Zhigang. (2021). A methodology for removing biofouling of the hull based on ultrasonic guided waves. Journal of Physics: Conference Series. 2031. 012006. 10.1088/1742- 6596/2031/1/012006.

Ishihara, H. (2017). Basic study on wall climbing root with magnetic passive wheels. 2017 IEEE International Conference on Mechatronics andAutomation, ICMA 2017, 1964–1969. https://doi.org/10.1109/ICMA.2017.8016119

K. Yoon and Y. Park, "Controllability of Magnetic Force in Magnetic Wheels," in IEEE Transactions on Magnetics, vol. 48, no. 11, pp. 4046- 4049, Nov. 2012, doi: 10.1109/TMAG.2012.2200240.

Lee, W. (2013). Proposition of reconfigurable wall climbing robot using 6DOF force torque sensor based on flexible structure for real environment. International Conference on Control, Automation and Systems, Iccas, 1802–1806. https://doi.org/10.1109/ICCAS.2013.6704232

M. Eich and T. Vögele, "Design and control of a lightweight magnetic climbing robot for vessel inspection," 2011 19th Mediterranean Conference on Control & Automation (MED), 2011, pp. 1200-1205, doi: 10.1109/MED.2011.5983075.

M. Tavakoli, C. Viegas, J. C. Romão, P. Neto and A. T. de Almeida, "Switchable magnets for robotics applications," 2015 IEEE/RSJ International Conference on Intelligent Robots and Systems (IROS), 2015, pp. 4325-4330, doi: 10.1109/IROS.2015.7353990.

V. Prabakaran et al., "Hornbill: A Self-Evaluating Hydro-Blasting Reconfigurable Robot for Ship Hull Maintenance," in IEEE Access, vol. 8, pp. 193790-193800, 2020, doi: 10.1109/ACCESS.2020.3033290.

Xu, Z. Y., Zhang, K., Zhu, X. P., & Shi, H. (2015). Design and optimization of magnetic wheel for wall climbing robot. Advances in Intelligent Systems and Computing, 363, 619–629. https://doi.org/10.1007/978-3-319-18997-0_54

.